

Feedback-Based Control Over the Spatio-Temporal Distribution of Arcs During Vacuum Arc Remelting *via* Externally Applied Magnetic Fields



MATT CIBULA, PAUL KING, and JOSH MOTLEY

Ampere Scientific's *VARmetric*TM measurement system for Vacuum Arc Remelting (VAR) furnaces passively monitors the distribution of arcs over time during VAR in real time. The arc behavior is known to impact both product yield and quality and can pose potentially catastrophic operating conditions. Arc position sensing with *VARmetric*TM enables a new approach to control the heat input to the melt pool. Transverse external magnetic fields were applied to push the arcs *via* the Lorentz force while measuring the arc location to control the arc distribution over time. This has been tested on Ampere Scientific's small-scale laboratory arc furnace with electromagnets used for control for up to 60 seconds while monitoring the arc location with *VARmetric*TM. The arc distributions were shown to be significantly different from the uncontrolled distributions with distinct thermal profiles at the melt pool. Alternatively, this type of control can be periodically applied to react to undesirable arc conditions.

<https://doi.org/10.1007/s11663-020-01959-w>

© The Minerals, Metals & Materials Society and ASM International 2020

I. INTRODUCTION

VACUUM Arc Remelting (VAR) furnaces are the workhorse for the manufacture of high value metals and alloys (Ni, Ti, Nb, Zr, Hf, *etc.*). During VAR, the input material (electrode) is lowered into a water-cooled copper crucible and heated under vacuum by an electric arc (50kW-5MW), the liquid metal drips into the crucible, and the molten pool solidifies into a homogeneous ingot.^[1] The controllable parameters of the solidification process, including the input heat (current and voltage), crucible dimensions, materials, and cooling rate, are critical to the production of defect-free homogeneous materials.^[2] These input parameters and associated boundary conditions control the properties of the molten pool, such as the pool depth, solidification angle, Rayleigh number, liquid velocity, and circulation time—all of which affect the persistence of defects, such as inclusions, freckles, white spots, *etc.*, into the final ingot.^[3] Despite the importance of producing defect-free ingots for safety-critical applications, including jet engines and medical implants, the VAR process has remained relatively unchanged since its introduction in the 1940s. Notable improvements in control include the

addition of cameras to visually monitor the melt around the annulus between the electrode and crucible wall, which improved safety during the melting process (by separating the operators from the furnace) while helping to better understand the arc dynamics *via* visual inspection^[4,5] and the introduction of drip-short control over the vertical position of the electrode.^[6,7] While drip-short control may provide more consistent melting and heating over time, it does not provide a mapping of the spatial distribution of heat at the surface of the melt pool, nor does it affect direct control over the location of the arcs which define the heat flux to the molten pool, two important parameters in providing full control over the solidification profile of VAR melted ingots. This paper addresses laboratory testing of the integration of arc position measurements with arc control utilizing a combination of the *VARmetric*TM measurement system (Figure 1) with transversely applied magnetic fields in order to provide spatial control over the arc distributions. The overall goal of this effort is to develop a full feedback system for arc distribution control for vacuum arc remelting.

II. BACKGROUND

The energy input for VAR is provided by a large (>5 kA) DC electrical current which bridges the gap between the electrode and the melt pool surface in the form of a vacuum arc. The current path through the furnace generates a magnetic field that changes over time as the arc moves around the electrode. Recently, methods

MATT CIBULA, PAUL KING, and JOSH MOTLEY are with Ampere Scientific, 1546 SW Industrial Way, Albany, OR 97322. Contact e-mail: matt@amprescientific.com
Manuscript submitted January 21, 2020.

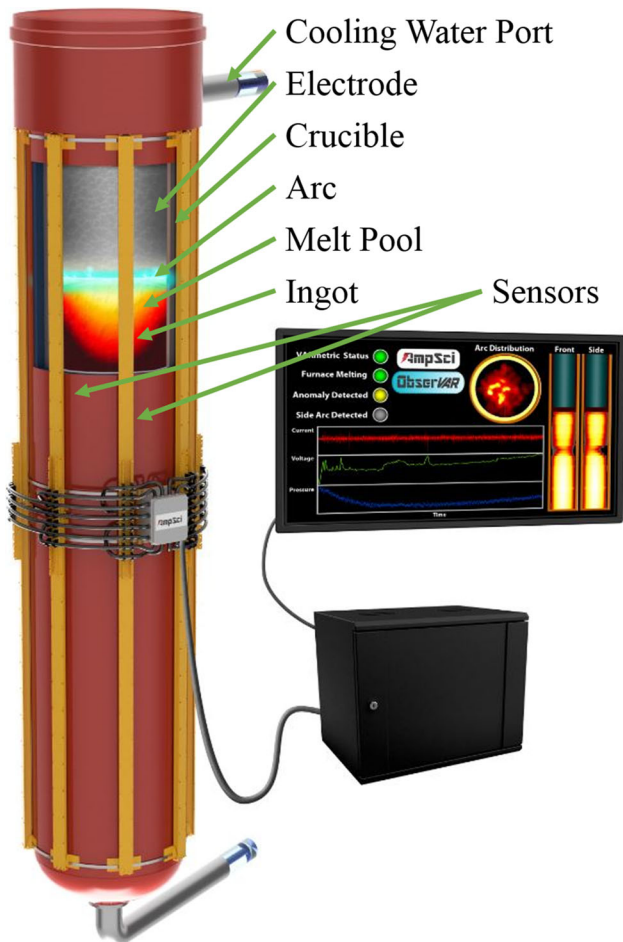


Fig. 1—VAR furnace with VARmetric™ sensors mounted to the exterior shell to monitor the distribution of arcs beneath the electrode.

utilizing measurements of the magnetic field to monitor the arc have been established to study the arc behavior.^[8,9] The Arc Position Sensing (APS) technology^[10] was initially proven at the National Energy Technology Laboratory, Albany, OR, and developed into the VARmetric™ measurement system, which performs continuous, real-time measurements of the arc during VAR hundreds of times per second.^[11] VARmetric™ combines an array of magnetic field sensors with simultaneous measurement of the furnace current and knowledge of the furnace's electrical geometry to calculate the centroid of the arc.^[12] This measurement can be utilized to generate a detailed map of the spatial distribution of the heat input to the melt pool. These results have already shown that the heat distribution is not generally axisymmetric about the center of the furnace or constant throughout the melt, in contrast to the typical parameters used in modeling solidification. For example, some computational models have shown that changing the heat distribution from a Gaussian shape to an annular shape may alter the solidification angle near the sidewall, impacting sidewall quality and ingot yield.^[2,5] Because most solidification models have assumed a static Gaussian, axisymmetric heat input, not

much is known about the correlation of these new measurements to the final ingot yield and quality. The few papers that relax axisymmetric or Gaussian assumptions indicate that the real-time arc dynamics have a profound effect on solidification models that cannot be predicted with these assumptions in place.^[13] For example, the Rayleigh number is used as an indicator of freckle formation, and transient models show 300 times increase due to thermal perturbations provided by a rotating arc.^[14] Utilizing only axisymmetric models, further examinations of this problem in relation to the types of changes in arc distributions that have been observed by VARmetric™ on an industrial furnace have shown a sensitive balance between the arc distribution and the ensuing solidification profiles.^[15]

Here, we present the development of the Vacuum Arc Control (VAC) technology which couples feedback from APS through VARmetric™ with externally applied transverse magnetic fields to directly control the arc location and thus providing a means of avoiding operational conditions leading to defects. Previous attempts to control the arc distribution in VAR with external transverse magnetic fields have only attempted to use a 'recipe'—such as a continuously rotating or switching magnetic field—to affect control over the arcs, but lacked information about the arc location and response to the applied fields.^[16,17] Axial magnetic fields applied to the furnace are often used as a process enhancement in VAR for certain alloys, but without regard to their impact on the arc distribution.^[18] They are typically intended to stir the melt pool to improve homogeneity in Titanium melting, but very few studies exist on how these applied fields modify the arc distribution in VAR. The VAC work presented here represents the first time that the authors are aware of where external magnetic fields have been applied to control arcs with simultaneous real-time magnetic-field-based measurements of the arc. At the stage of development reported here, the system required a human operator to monitor APS and control the electromagnets. Despite this, the capabilities of the VAC proven here are evidence that a closed loop controller is now possible.

III. EXPERIMENTAL VACUUM ARC FURNACE

The experimental VAR system was designed to emulate the physical and operational conditions of an industrial scale VAR at a research scale. Figure 2 shows the physical apparatus, including the vacuum chamber, vacuum pump, gas feed valve, horizontal adjustment feedthroughs, electrodes, electrical input and output feedthroughs, and a 15 kW (0 to 510 A, 0 to 80 V) power supply. This system was supplemented with VARmetric™ to monitor the arc location in real time at 150 Hz; synchronized video cameras to visually confirm the arc location measurements; and a pressure transducer for vacuum measurements. The system was configured with a fixed lower electrode and a movable upper electrode to draw the arc to a fixed gap size of up to 3 cm. The electrodes are copper (upper) and stainless steel (lower)

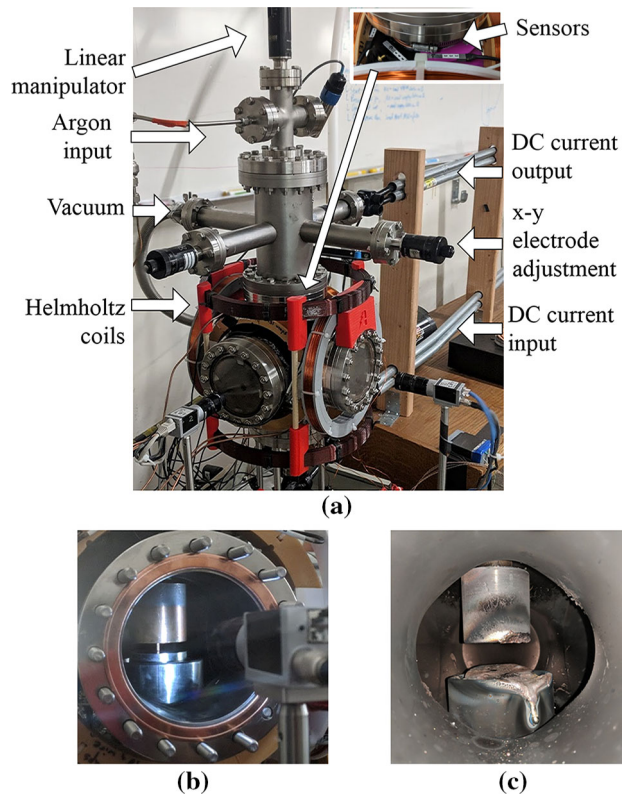


Fig. 2—(a) Arc furnace arrangement including 3-axis Helmholtz coils, with the inset showing VARmetric™ sensor locations. (b) Copper and steel electrodes configured with a copper bridge to calibrate sensors. (c) Electrodes upon completion of a test.

cylinders with 5.08 cm diameter surfaces, although for longer duration tests, the lower electrode was extended to include a 7.62 cm diameter drip cup to contain liquid metal. This scale was chosen to keep the density of arcs on the electrode surface similar to industrial conditions. Assuming 70 A/arc, the experimental furnace provides an arc density of 0.044-0.088 arcs/cm², while industrial furnace may melt up to 100 cm diameter electrodes with 5 to 50 kA, resulting in a typical arc density between 0.0091 and 0.36 arcs/cm². Therefore, in terms of spacing between arcs, the experimental arc furnace is within the industrial operating regime for VAR.

Arcs within the furnace can typically be defined as diffuse, constricted, or semi-constricted. A spatially diffuse arc is shown in Figure 3(a)—over the exposure time, 6 ms, there appears to be a single dim arc column, whose width nearly covers the entire electrode. The centroid measured on this type of arc appears as a slowly varying, confined spot near the center of the electrode. Alternatively, a semi-constricted arc distribution (Figure 3(b)) is composed of a few constricted columns, approximately 1 cm in diameter during an exposure. The cathode spots and their plasma columns move rapidly across the surface of the electrode, typically moving out from the center and traveling up the side of the electrode before extinguishing. In this mode, when two or more cathode spots were beneath the electrode, simultaneously, they repelled each other,

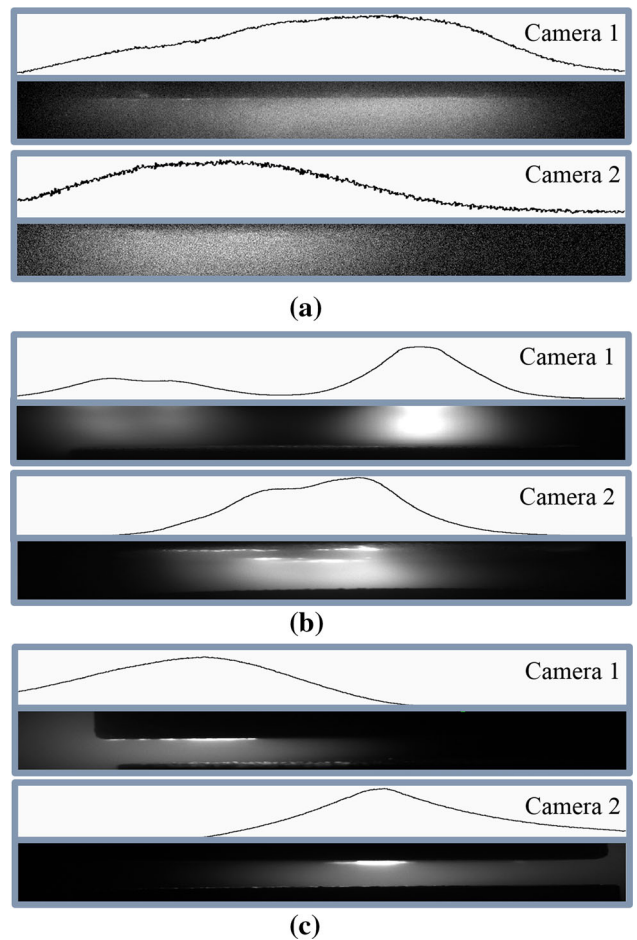


Fig. 3—(a) Diffuse, (b) semi-constricted, and (c) constricted arcs over 5.08 cm diameter electrodes with a 1 cm gap. Images taken with a 6 ms exposure time.

exhibiting retrograde motion in response to the self-magnetic field that is typical of vacuum arcs.^[19] Finally, for a constricted arc (Figure 3c), all of the arc columns are focused to a tight (1 to 2 cm) region on the electrode for an extended period of time (>5 seconds). All the conditions shown in Figure 3 were captured approximately 1-10 seconds after ignition of the arc on cold electrodes. At this time, the electrode surfaces are well below the thermionic emission temperature, but over longer time periods (up to 90 seconds), the electrodes reached the melting temperature of the material and the arc dynamics are expected to change over time during these tests as the electrode surface conditions change.

The experimental apparatus was designed with two independent methods of determining the location of the arcs, either by image analysis from two orthogonally oriented cameras, or by utilizing APS with VARmetric™, see Appendix A. Figure 4 gives an example of these measurements over a sequence of captured images. The ‘single-arc’ method of APS applies the Biot-Savart law to calculate the arc centroid from electromagnetic measurements of the furnace.^[9] Because the VARmetric™ sensors are placed in close proximity to the electromagnets, they

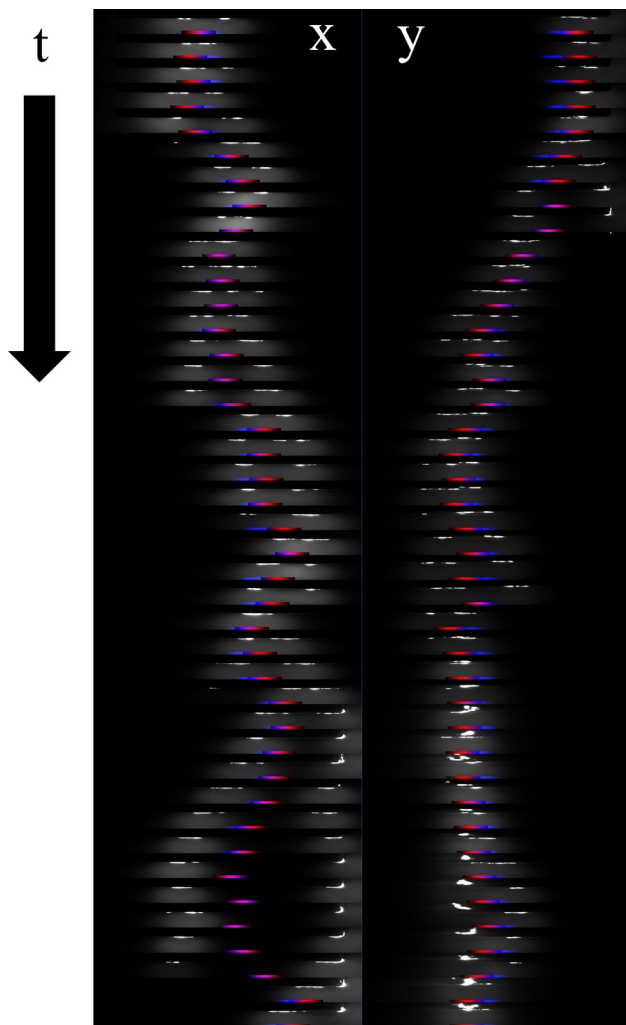


Fig. 4—Image sequences from cameras oriented along the (x) and (y) axes showing the motion of the arc distribution frame by frame. The blue and red hashes (purple when overlapping) show the APS calculated and image intensity measurements of the centroid, respectively, for each frame. The APS measurement provides the feedback required for a closed loop control system over the arc distribution in VAR. Note how as the arc columns separate, both APS and image analysis methods calculate the centroid of the arc in between the arc columns. In the final few frames, one of the two arc columns extinguishes and the centroid shifts to the single remaining column. This shift begins as the intensity of the extinguishing column reduces, indicating that the total current in the extinct column decays over time before extinguishing (Color figure online).

require additional calibration which uses an external measurement of the electromagnet current to subtract out the applied field.

APS was initially developed to calculate the location of an electric current residing in the same plane as the magnetic sensors used for detection; however, the method was extended to 3D to detect arcs above or below the sensor plane, but within the volume bordered by the sensors.^[20] With the 3D methodology, the sensors shown in Figure 2, for example, can be used to accurately calculate the centroid of the vacuum arc in

the arc gap approximately 10 cm below the sensing plane. Similarly, video images are analyzed to determine the arc centroid by measuring the center of mass of the light intensity distribution emitted by the plasma beneath the electrode (Figure 5(a)). Only one non-unique case exists for the calculated arc centroid: a completely random distribution of many arc columns over the surface of the electrode, a homogeneous glow discharge, and a centered constricted arc would all result in a measurement of the centroid of the arcs at the center of the electrode. These cases are only distinguishable with APS by higher order statistical and temporal measurements, but image analysis of the arcs in the gap provides a simpler method to determine the arc structure in this furnace. For tests ranging from 10 to 60 seconds, with 1500 to 9000 measurements, the correlation coefficient between the APS and video was > 0.95 , indicating good agreement between the two measurements (Figure 5(b)). Figures 5(c) and (d) provide a comparison of the measured arc distributions over time for each method with the furnace current set to 500 A and 250 A. The 2D distribution plots were produced by treating the arc as a Gaussian distribution of current around the centroid location, with a full width at half max diameter of 1 cm for each data point collected. The 2D sum of all frames was then used to generate a heat map of the total distribution of arcs over a given time period by mapping colors in the order [black–red–yellow–white], where white is the maximum value. This treatment approximates the thermal power distribution at the melt pool surface in a VAR. At 500 A, the distribution is concentrated to the center of the electrode. This is attributed to the increased number of arcs in the semi-constricted mode, which tend to average out the calculated arc centroid towards the center of the furnace. Additionally, in some tests, at 500 A the arc locked into a constricted mode and ‘stuck’ to one side of the electrode—in these cases the arc distribution reflected this observation. The measurement of the arc location is essential for effective control because the arc response to an external magnetic field is known to be highly dependent on the gap size, materials, geometry, temperature, current, and magnetic field.^[19]

IV. VACUUM ARC CONTROL

In order to push the arcs with an external magnetic field, a 3-axis Helmholtz coil system was designed to apply uniform fields (-40 to 40 Gauss, >92 pct uniformity) in a 5.08 cm diameter sphere around the center of the furnace. The fields were generated with a set of switching DC power supplies, which were able to reverse the direction of the field within 0.1 second. Due to the principal of superposition, this configuration makes it possible to produce a uniform field in any direction throughout the entire volume of the arc gap. The uniform nature of the field within the arc gap was designed to apply a similar and predictable force to an

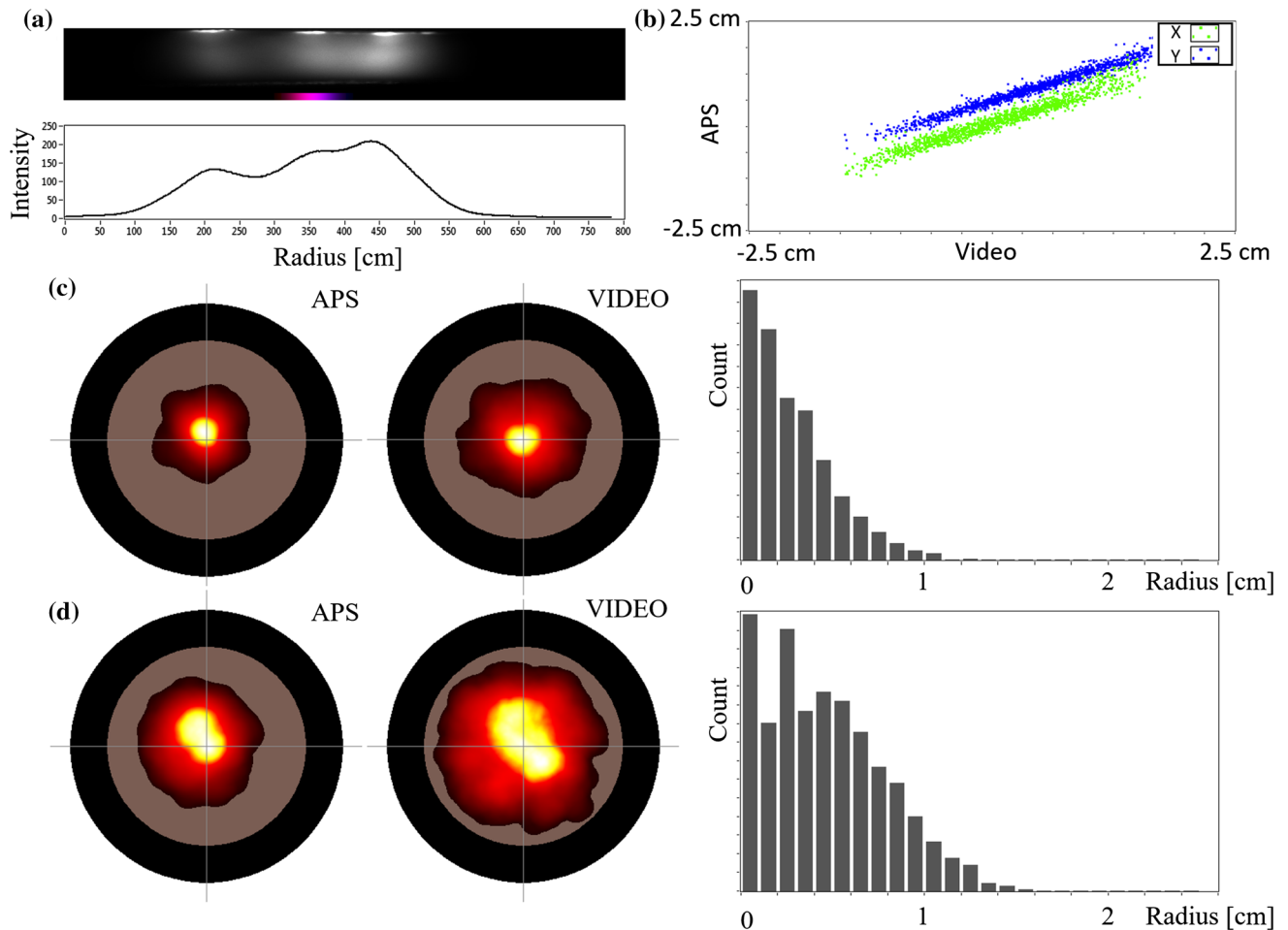


Fig. 5—Comparison between measurements of the arc centroid taken by VARmetric™ and by image processing. (a) Image taken by one of the cameras and the arc luminosity measured within the gap, showing the centroid measurement overlaid on the image. (b) Correlation between APS and luminosity centroid measurements over 20 s of arc location measurements. The shift between the measurements here is attributed to measurement error in the calibration of one of the cameras to the spatial position of the electrodes. Rows (c) and (d) compare the arc distributions and centroid measurements for an uncontrolled arc at 500 Amps and 250 Amps. The outer black ring extends to the edge of the 7.62 cm diameter drip cup, while the copper ring extends to the edge of the 5.08 cm diameter electrode surfaces.

arc column in any location across the electrode. While multiple simultaneous arc columns exhibited retrograde motion and repelled each other under the uncontrolled, cold cathode state, the external magnetic fields pushed the arcs in the direction of the Lorentz force. The range of applied field strength is on the same order of magnitude as the stirring coils used on some industrial furnaces, which are known to affect the distribution of arcs beneath the electrode, as well as apply forces to stir the melt pool, by applying a uniform field along the longitudinal axis of the furnace with a solenoid.

Figure 6 provides a diagram of the feedback loop developed for this application. The arc distributions measured by VARmetric™ are fed through the vacuum arc controller in order to provide an estimate of the magnetic field estimate required to move the arc. This estimate is then utilized to energize the Helmholtz coils to actuate the control. Additionally, the magnetic fields associated with the Helmholtz coil and any other

external sources are accounted for through either direct measurement or field calibration so that the desired fields from the arc are isolated. Finally, for these experiments, manual override was performed while tailoring the arc distribution, and thus, the experiments did not provide true feedback control. However, the goal of this effort was to show the efficacy of the process leading towards full feedback control.

Figure 7 shows the effect of a static transversely oriented magnetic field on the distribution of arcs over 10 seconds compared to an uncontrolled arc. Prior to activating the translational control of the arc, the camera images show a semi-constricted arc with 1 to 3 columns that move across the parallel surfaces. Meanwhile, the arc distribution is nearly centered and spread out and covers most of the electrode surface. Histograms of the arc radius and angle measurements show a broad distribution, indicating that the arc is moving freely about the electrode as might be expected. After

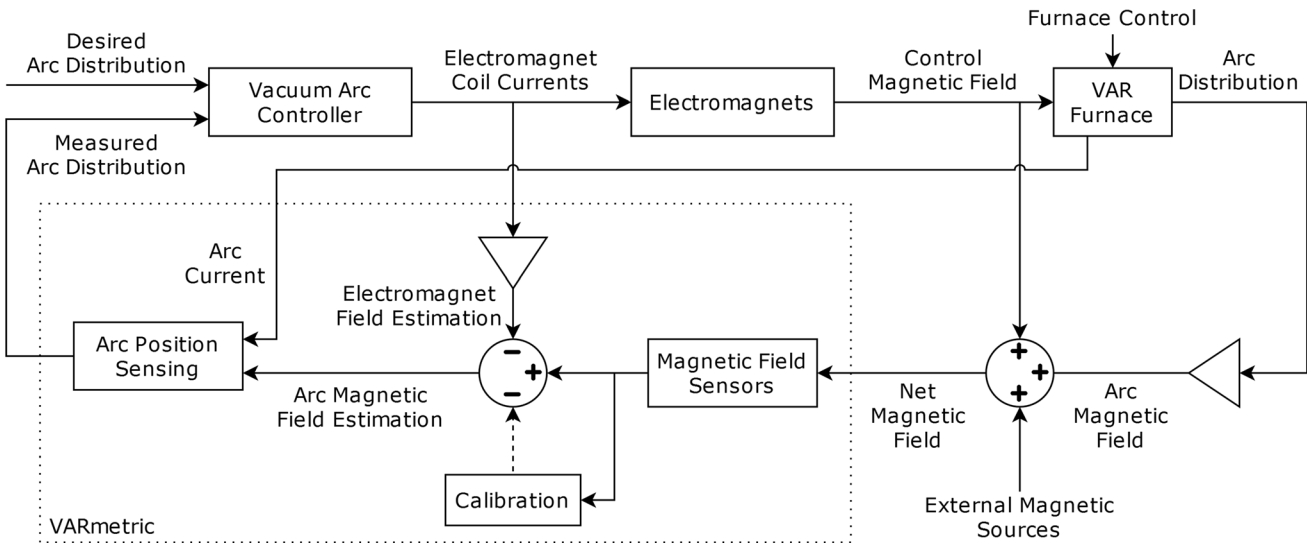


Fig. 6—Feedback loop for Vacuum Arc Control where the difference between the measured and desired arc distributions are evaluated in order to engage the Helmholtz coils. Here, the VARmetric™ measurement system is identified within the dotted box, providing the arc distribution measurement at a rate of 150 Hz. For our experiments, the Measured Arc Distribution was not fed back to the VAC, rather the operator provided a manual override in order to drive the arc distributions to the desired states.

applying the control field, the arc moves predictably in response to the Lorentz force, F_L , to one side of the electrode and remains focused at that location. Arc radius and angle are commensurately constricted as indicated in the histograms. This action was verified with at least 30 tests at varying control field strengths and directions. At higher field strengths, it was possible to extinguish the arc by pushing the arc to the edge of the electrode, while at lower levels, the average radial position of the arc centroid was reduced. It should be noted that unlike an industrial VAR, this arc furnace does not have crucible sidewalls that could conduct the arc beyond the edge of the electrode, so it might be expected that this behavior could push the arc from the melt pool to the sidewall or vice versa. While this system exhibited Amperian motion, an industrial VAR may have a retrograde response to the applied field. However, the information provided by VARmetric™ will enable a controller to adapt to any response that the arc may have to the applied fields.

Using the transverse magnetic field, the distribution of the arc over time was continuously controlled by switching the orientation of the magnetic field every second between 8 different directions over 180 deg. The results for each control step are provided in Figures 8(a), while (b) shows how the total controlled arc distribution over 8 seconds compares to an uncontrolled distribution, (c), over the same time frame in the same melt. While the uncontrolled arc forms a Gaussian-type distribution around the center of the electrode, the control fields focus the arc off-center to about 2/3 of the electrode radius and push the arc around the electrode. Similar arc distributions have been measured by VARmetric™ on industrial titanium alloy VAR furnaces, for example. However, in this case, the arc distribution was controlled, and the arcs moved in the direction expected by the Lorentz force for each field direction.

V. CONCLUSIONS

This paper presents results of utilizing a synchronized measurement system to measure and control arc locations and more importantly arc distributions, as a function of time. A purpose-built experimental vacuum arc remelting furnace was constructed to accommodate VARmetric™ and the Arc Position Sensing technology as well as the Vacuum Arc Control mechanism to exacting laboratory standards for accuracy in measurements. The VAC comprised a series of orthogonally oriented Helmholtz coils designed to provide a uniform field in a specified direction at the center of the VAR and across the electrode area. By actuating the orthogonal fields, the resultant control force vector is completely tailorable in 3D with response characteristics in the millisecond time frame, enabling continuous control of the arc over time.

While the type of control demonstrated here did not utilize active automated feedback from the APS and required a human operator, further developments in the hardware and software for the test furnace enabled longer melting (up to 90 seconds at 500 Amps) and real-time control over the applied field. The user interface for the controller software (Figure 9(a)) enabled the user to choose the direction and strength of the desired force with the computer mouse and hence provide a corresponding field from the Helmholtz coils to accommodate the desired force. This controller interface was provided with a real-time arc distribution plot so that the user could act in response to changes in the arc distribution. The tests proved that this type of control enabled the user to ‘push’ the arc out of constrictions and apply more uniform heating to the surface of the electrode, while uncontrolled arcs frequently stuck to one side of the electrode and rapidly melted the surface in that region.

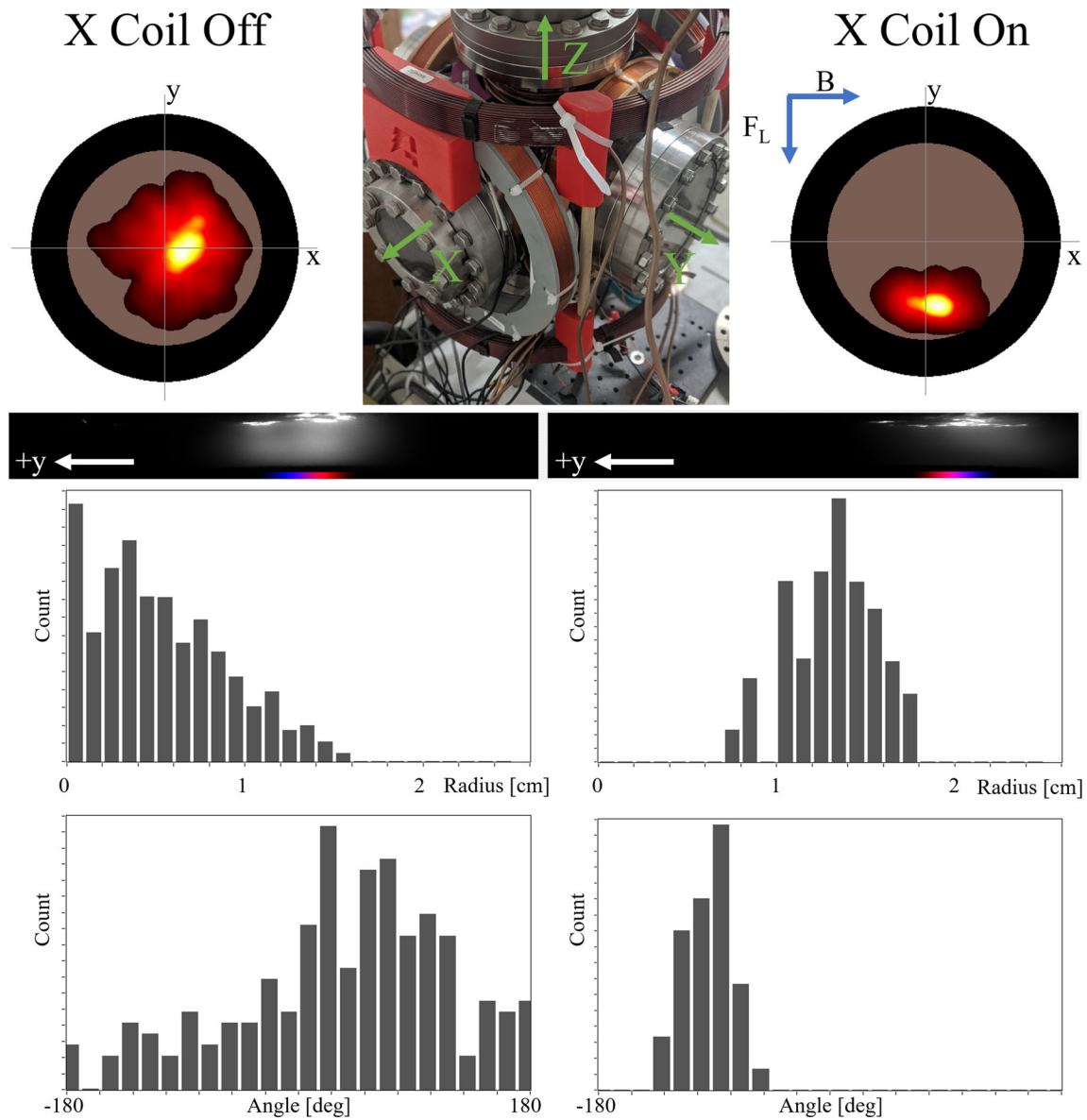


Fig. 7—Arc distribution before (left) and after (right) applying a uniform, transverse magnetic field to the arc gap in the x -direction with the 3-axis Helmholtz coil system. Initially, the arc was free to roam about the 5.08 cm diameter electrodes, but after the control was applied, the arc moved in the direction of the Lorentz force. For the duration of these tests, the arc remained pinned to that side of the electrode until the control field was changed.

Ampere Scientific continues the development of the *VARmetric* + VAC on an industrial furnace under funding provided by the National Science Foundation. Implementation of the industrial trials are to begin in late 2020 where feedback from *VARmetric*TM will be integrated with the VAC to control arc distributions and consequently the heat flux for segregation prone alloys. In parallel, solidification modeling is being used to predict pool shape as a function of heat flux towards development of an integrated tool able to measure, predict, and control solidification as a function of heat

flux where, for example, the instantaneous arc distributions over time are used to provide feedback for the control algorithm.

ACKNOWLEDGEMENTS

We wish to acknowledge the deep insights into Arc Position Sensing provided by Dr. Rigel Woodside without whom this body of work could not have been

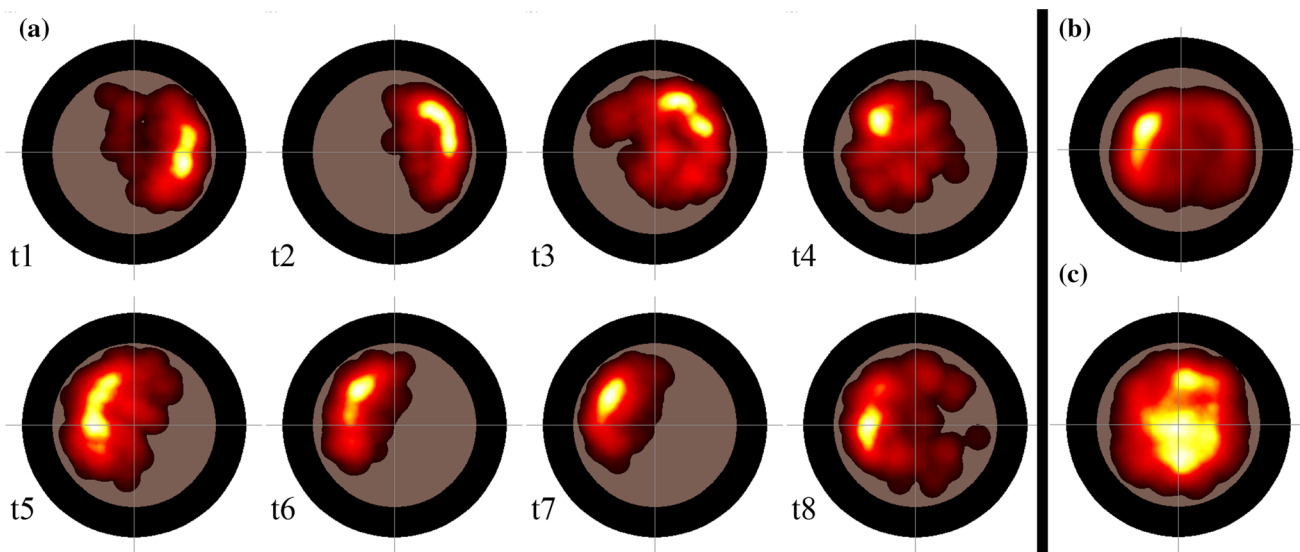


Fig. 8—(a) Arc distributions, each of which shows 1 s of measurements, over a total of 8 seconds for a controlled arc as the control field is rotated around 180 deg. The direction of the Lorentz force is indicated by the overlaid arrow for each time step. The total arc distribution over the 8 s control, (b), shows that the arc spends more time near the edge of the electrode than an uncontrolled arc distribution over the same time period, (c).

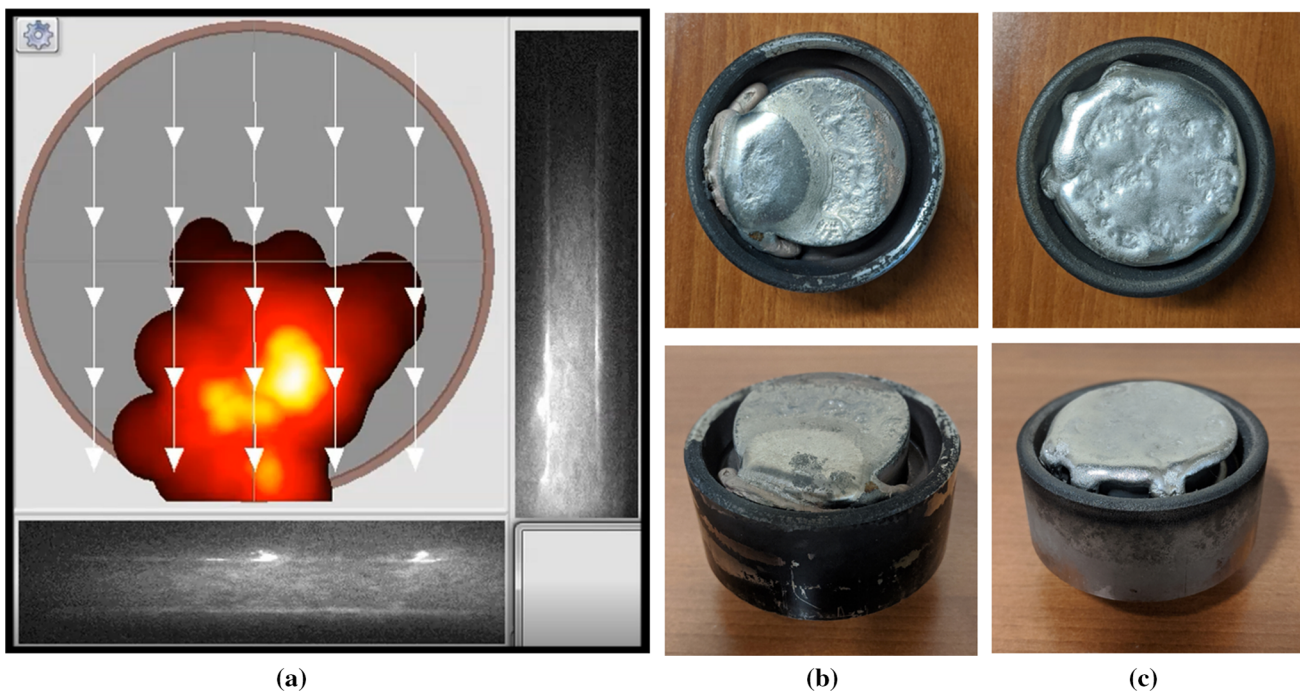


Fig. 9—(a) User interface to enable control over the arc distribution with simultaneous real-time monitoring. The user is able to click and drag the mouse on the display to change the strength and orientation of the vector indicating the Lorentz force applied. (b) and (c) show the cooled lower electrode after running the furnace for 60 s at 500 A, without (b) and with (c) the user applying the VAC to provide uniform heating.

completed. Some or all of this work was supported by the National Science Foundation SBIR Phase I Grant Number 1647655 and the National Science Foundation SBIR Phase II Grant Number 1831255 as well as Business Oregon Grant Numbers C2018096 and C2018335. We are greatly appreciative of the support

provided by the National Science Foundation and Business Oregon in support of our efforts. Additionally, we would like to acknowledge the discussions and contributions provided by Dr. Gordon Alanko of ATI Specialty Alloys, Mr. Warren George (ret), and Dr. Rodney Williamson (ret) for the insightful discussions

and Mr. Nathan Pettinger and Mr. Brad Anderson for contributions to the project.

APPENDIX A—*VARMETRIC*TM

*VARmetric*TM capitalizes on the Biot–Savart Law relating the magnitude and direction of a magnetic field to the electric current source generating it. As magnetic fields behave under the principal of superposition, the current source of interest can be obtained by isolating that source from other sources in the area:

$$\vec{B} = \vec{B}_A + \vec{B}_C + \vec{B}_E + \vec{B}_I + \vec{B}_F \quad [\text{A1}]$$

For us, \vec{B}_A is the magnetic flux density due to the current, I is flow within an arc at a location P, while \vec{B}_C , \vec{B}_E , \vec{B}_I and \vec{B}_F are external sources not of interest and include the fields from the crucible, electrode, ingot, and other external sources. For the purpose of this analysis, we recognize that the other sources are static with the exception of small changes in current distribution as a function of changes in the arc position. The arc is moving much faster than the other sources and so we can ignore the magnetic field flux due to these sources. In the plane of the arc, \vec{B}_A is then given in cartesian coordinates as $\vec{B}_A = B_x \hat{i} + B_y \hat{j}$ by treating the arc as a current line source:

$$B_x = m_x I \left(\frac{\sin(\theta)}{r} - a \right); \quad B_y = m_y I \left(\frac{\cos(\theta)}{r} - b \right) \quad [\text{A2}]$$

where B_x and B_y are the x and y components of the magnetic flux at P. We note here that in these equations, the coefficients m_x , m_y , a , and b are relaxed from the field of a current line source, where $m_x = m_y$ and $a = b$; this has the effect of coupling the crucible's and electrode's current dependence on arc location back into the arc field. These equations can be solved analytically for r and θ , if the coefficients m_x , m_y , a , and b are known:

$$r = \left[\left(\frac{B_y}{m_y I} + b \right) * \left(\left[\left(\frac{B_x}{m_x I} + a \right) \right]^2 + 1 \right)^{\frac{1}{2}} \right]^{-1} \quad [\text{A3}]$$

$$\tan(\theta) = \frac{\left(\frac{B_x}{m_x I} + a \right)}{\left(\frac{B_y}{m_y I} + b \right)} \quad [\text{A4}]$$

As previously reported for Arc Position Sensing,^[12] the coefficients are evaluated based upon a computational sweep of potential geometrical changes in the system (*e.g.*, differing arc locations across the arc gap) where a curve fit is utilized to provide a functional relationship for m_x , m_y , a , and b , based upon the arc location. In practice, some of the external field sources are naturally included in the computational model, so that these coefficients account for all fields produced by the furnace.

REFERENCES

1. R. Boxman, D. Sanders and P. Martin, Handbook of Vacuum Arc Science & Technology: Fundamentals and Applications, William Andrew, 1996.
2. A. Mitchell: *Mater. Sci. Eng. A*, 2005, vol. 413, pp. 10–18.
3. F. Zanner, R. Williamson and R. Erdmann, *LMPC 2005 - Proc. 2005 Int. Symp. Liquid Metals Processing and Casting, Santa Fe, NM*, PD Lee et al., Ed., ASM International, 2005, pp. 13–27.
4. P. Chapelle, C. Noel, A. Risacher, J. Jourdan, A. Jardy, and J. Jourdan: *J. Mater. Proc. Tech.*, 2014, vol. 214 (11), pp. 2268–75.
5. R. M. Ward, B. Daniel and R. Siddall, *LMPC 2005 - Proc. 2005 Int. Symp. Liquid Metals Processing and Casting, Santa Fe, NM*, PD Lee et al., Ed., ASM International, 2005, pp. 49–56.
6. J. Beaman, L. Lopez, and R. Williamson: *J. Dyn. Sys. Meas. Cont.*, 2014, vol. 136 (3), p. 031007.
7. F.J. Zanner: *Met. Trans. B*, 1981, vol. 11 (3), pp. 721–28.
8. R. Ward and M. Jacobs: *J. Mater. Sci.*, 2004, vol. 39 (24), pp. 7135–43.
9. R. Woodside and P. King, *LMPC 2009 - Proc. 2009 Int. Symp. Liquid Metals Processing and Casting, Santa Fe, NM*, PD Lee et al., Ed., ASM International, 2009, pp. 75–84.
10. R. Woodside and P. King, *Int. Inst. Meas. Tech. Conf. Proc.*, 2010, pp. 452–57.
11. M. Cibula, R. Woodside and P. King, in *LMPC 2017 - Proc. 2017 Int. Symp. Liquid Metals Processing and Casting*, 2017, pp. 25–30.
12. R. Woodside, P. King, and C. Nordlund: *Met. Trans. B*, 2013, vol. 44 (1), pp. 154–65.
13. K. Pericleous, G. Djambazov, M. Ward, L. Yuan, and P. Lee: *Met. Trans. A*, 2013, vol. 44 (12), pp. 5365–76.
14. L. Yuan, G. Djambazov, P.D. Lee, and K. Pericleous: *Int. J. Mod. Phys. B*, 2009, vol. 23 (6), pp. 1584–90.
15. J. Motley, K. Kelkar, P. King, M. Cibula and A. Mitchell, *LMPC 2019 - Proc. 2019 Int. Symp. Liquid Metals Processing and Casting*, 2019, pp. 17–28.
16. D. R. Mathews and R. J. Krieger, US Patent 4581745A, 08 04 1986.
17. S. Ogino, S. Inoue, T. Tomai and M. Tamura, US Patent 4762165, 09 08 1988.
18. P. Chapelle, A. Jardy, J.P. Bellot, and M. Minvielle: *J. Mater. Sci.*, 2008, vol. 43, pp. 5734–46.
19. M. Drout: *IEEE Trans. Plasma Sci.*, 1985, vol. 13 (5), pp. 235–41.
20. M. Cibula, P. King and C. Woodside, US Patent US10514413B2, 12 24 2019.

Publisher's Note Springer Nature remains neutral with regard to jurisdictional claims in published maps and institutional affiliations.